# Modulation of whistler mode chorus waves: 2. Role of density variations

W. Li,[1] J. Bortnik,[1] R. M. Thorne,[1] Y. Nishimura,[1,2] V. Angelopoulos,[3] and L. Chen[1]

Received 1 December 2010; revised 1 February 2011; accepted 21 March 2011; published 9 June 2011.

[1] Modulation of whistler mode chorus waves, which plays an important role in driving the pulsating aurora and other processes related to energetic electron dynamics, is an interesting but a long-standing unresolved problem. Here we utilize in situ observations from the THEMIS spacecraft to investigate the role of density variations in the modulation of the chorus wave amplitude, which forms a complementary study to the modulation of chorus by compressional Pc4–5 pulsations presented in a companion paper. We show that these density variations are correlated remarkably well with modulated chorus intensity and typically occur on a timescale of a few seconds to tens of seconds. Both density depletions (DD) and density enhancements (DE) are frequently correlated with increases in chorus wave amplitudes. Furthermore, density enhancements cause a lowering of the central frequencies of the generated chorus waves and vice versa. DD events are more likely to be related to quasi-periodic chorus emissions and thus may be related to the generation of the pulsating aurora. A systematic survey of both DD and DE events shows that DD events preferentially occur between premidnight and dawn, whereas DE events dominantly occur from dawn to noon. We also evaluate the growth rates of chorus waves using linear theory for both DD and DE events and show that both density depletions and enhancements can lead to an intensification of chorus wave growth. However, other potential mechanisms for chorus intensification caused by density variations such as wave trapping by density crests and troughs cannot be excluded.

**Citation:** Li, W., J. Bortnik, R. M. Thorne, Y. Nishimura, V. Angelopoulos, and L. Chen (2011), Modulation of whistler mode chorus waves: 2. Role of density variations, *J. Geophys. Res.*, *116*, A06206, doi:10.1029/2010JA016313.

## 1. Introduction

[2] Whistler mode chorus waves have received increased attention recently, due to their important roles in both acceleration and loss of energetic electrons in the inner magnetosphere. Chorus waves contribute significantly to the stochastic acceleration of electrons up to relativistic energies through efficient energy diffusion [*Horne and Thorne*, 1998; *Summers et al.*, 2002; *Meredith et al.*, 2002; *Horne et al.*, 2005a, 2005b; *Shprits et al.*, 2006; *Bortnik and Thorne*, 2007; *Chen et al.*, 2007; *Li et al.*, 2007; *Shprits et al.*, 2009; *Subbotin et al.*, 2010]. Pitch angle scattering by chorus waves leads to a net removal of energetic electrons from the outer radiation belt and causes intense microburst precipitation of relativistic electrons [*Lorentzen et al.*, 2001; *O'Brien et al.*, 2004; *Thorne et al.*, 2005; *Bortnik and Thorne*, 2007]. Whistler mode chorus can also scatter plasma sheet electrons with energy between a few hundred eV and tens of keV into the atmosphere and form commonly observed diffuse aurora [e.g., *Horne et al.*, 2003; *Ni et al.*, 2008; *Thorne et al.*, 2010]. The generation of quasi-periodic chorus emissions with a fairly well defined periodicity results in the precipitation of energetic electrons [e.g., *Kennel and Petschek*, 1966; *Lepine et al.*, 1980], which also exhibits modulation on the same timescale, and is observed on the ground as the pulsating aurora [e.g., *Johnstone*, 1978, 1983; *Davidson*, 1990; *Miyoshi et al.*, 2010; *Nishimura et al.*, 2010].

[3] It is generally accepted that chorus is excited during cyclotron resonant interaction with anisotropic plasma sheet electrons [e.g., *Kennel and Petschek*, 1966; *Helliwell*, 1967; *Nunn et al.*, 1997; *Omura et al.*, 2008], which are injected into the inner magnetosphere during geomagnetically active times [*Burtis and Helliwell*, 1969; *Tsurutani and Smith*, 1974; *Meredith et al.*, 2001, 2003; *Li et al.*, 2009]. However, the mechanisms responsible for the formation of the quasi-periodic spectrum of whistler emissions on a timescale of a few seconds to tens of seconds are still a subject of active research [e.g., *Sazhin and Hayakawa*, 1992, 1994, and references therein]. *Coroniti and Kennel* [1970] connected the quasi-periodic whistlers with the modula-

[1]Department of Atmospheric and Oceanic Sciences, University of California, Los Angeles, California, USA.
[2]Solar-Terrestrial Environment Laboratory, Nagoya University, Nagoya, Japan.
[3]Institute of Geophysics and Planetary Physics, Department of Earth and Space Sciences, University of California, Los Angeles, California, USA.


0148-0227/11/2010JA016313

tion of the linear growth rates caused by geomagnetic pulsations. Using OGO-5 observations in the equatorial magnetosphere, *Tsurutani and Smith* [1974] pointed out that chorus emissions are of burst-like nature with the bursts often occurring at quasi-periodic intervals from ~3 s to a few minutes. Although variations of the ambient magnetic field were observed during quasi-periodic events, no apparent correlation between chorus pulsations and micropulsations were detected [*Tsurutani and Smith*, 1974]. *Davidson* [1979] proposed a model of self-modulated pulsations of whistler waves and electron fluxes, demonstrating that if too many electrons are removed by wave interactions, the system restores itself by building up the flux to values exceeding the equilibrium flux, repeated through many cycles. More recently, *Pasmanik et al.* [2004] using a self-consistent simulation of the cyclotron instability showed that the generation regime of self-sustained pulsations could explain quasi-periodic whistler wave emissions. Despite these previous studies, the causative mechanism of quasi-periodically modulating whistler waves has not reached a general agreement yet.

[4] The role of density in modulated whistler waves has been reported in a few previous studies. Satellite observations [*Angerami*, 1970; *Koons*, 1989; *Moullard et al.*, 2002] showed that whistlers can be guided by field-aligned ducts of both density enhancements and depletions. *Scarf and Chappell* [1973] reported the first simultaneous observations of lightning-generated whistler waves together with ambient plasma density measurements and found that the majority of ducts were density enhancements whereas a small portion were density troughs. *Koons* [1989] demonstrated that strong enhancements of whistler mode emissions were correlated with plasma density enhancements (>40%) in the outer plasmasphere between $L = 4$ and $L = 6$, indicating that these density enhancements act as whistler mode wave ducts. *Angerami* [1970], using whistler dispersion data collected by the OGO 3 satellite, concluded that density enhancements in whistler ducts generally lie between 6% and 22% and rarely exceed 33% of the background density. Furthermore, whistler wave packets associated with density cavities were detected in the auroral zone on the Freja satellite [*Huang et al.*, 2004]. More recently, *Moullard et al.* [2002] reported that whistler mode waves were modulated by density fluctuations during a plasmapause crossing event near the geomagnetic equator. However, most previous studies reported on the modulation of whistler waves by density variations inside plasmasphere or close to the plasmapause or at high geomagnetic latitudes. Studies dealing with the modulation of chorus waves by density variations outside the plasmapause in the equatorial magnetosphere are very limited.

[5] Propagation of whistler waves in density inhomogeneities has previously been studied through theory and simulation. *Smith* [1961] proposed a theory showing that both density enhancements and depletions can trap whistler waves under certain conditions. *Gorney and Thorne* [1980] compared the ducting ability of various density structures and concluded that modest (20%) perturbations are capable of effective ducting. More recently, *Streltsov et al.* [2006] investigated whistler propagation in magnetic field-aligned channels (also called ducts) with either enhanced or depleted plasma density under situations where the transverse scale size of the duct is comparable to or smaller than the perpendicular wavelength of the whistler. They found that both enhanced and depleted plasma densities can lead to the intensification of chorus whistler wave amplitudes. Ducts caused by density variations would substantially alter the paths of propagation of the whistler waves. Despite previous studies on whistler wave trapping in density depletions and/or enhancements, the mechanism of whistler wave modulation still needs further investigation.

[6] The main objective of this study is to examine the role that plasma density variations play in the modulation of chorus waves. Using simultaneous wave and density data (inferred from the spacecraft potential) from THEMIS in the near-equatorial magnetosphere we focus on timescales from a few seconds to tens of seconds. Longer-time modulation of whistler mode chorus, in the Pc4–5 range, is discussed in a companion paper by *Li et al.* [2011]. We sort the events into two categories; chorus modulation by (i) density depletions (DD) and (ii) density enhancements (DE). We investigate how well the chorus modulation in each category can be explained by the changes in the linear wave growth rate. In Section 2, two DD events and two DE events are analyzed in detail, followed by a statistical analysis of the global distribution of each type of event. In Section 3 we analyze the variation of linear growth rates for each type of event and compare our results to the observed wave intensity change. In Sections 4 and 5 we discuss and summarize the principal results of the present study.

## 2. Observational Results

[7] The THEMIS data set used in the present study has been described in detail in *Li et al.* [2011], and only a brief summary is included below for convenience. All data used in this study are from the THEMIS spacecraft, including wave electric and magnetic fields from the Electric Field Instrument (EFI) and Search Coil Magnetometer (SCM), electron distributions from Electrostatic Analyzer (ESA) and Solid State Telescope (SST), background magnetic field data from Fluxgate Magnetometer (FGM). Total electron density used in this study is inferred from the spacecraft potential. Since the present paper investigates chorus modulation on a timescale of a few seconds to tens of seconds, all data used is obtained during the interval when particle burst data is available in order to get the wave data with high resolution in time and frequency. These THEMIS data have been utilized to investigate the role of density variations in the modulation of chorus wave amplitudes in the dominant chorus source region.

### 2.1. Correlation Between Density Depletion and Chorus Intensification

[8] We begin by presenting two DD events that were recorded when the particle burst data was available. Figure 1 shows an overview of the properties of the plasma associated with chorus modulation observed on 15 October 2008 as THEMIS E traversed the typical chorus source region [e.g., *Tsurutani and Smith*, 1974; *Meredith et al.*, 2003] located at ~6.5 MLT and 5.9 $R_E$. Time-frequency spectrograms of wave electric (Figure 1h), magnetic field wave spectral intensity (Figure 1i), and integrated wave magnetic field amplitude for lower band chorus over the frequency range 0.05–0.5 $f_{ce}$

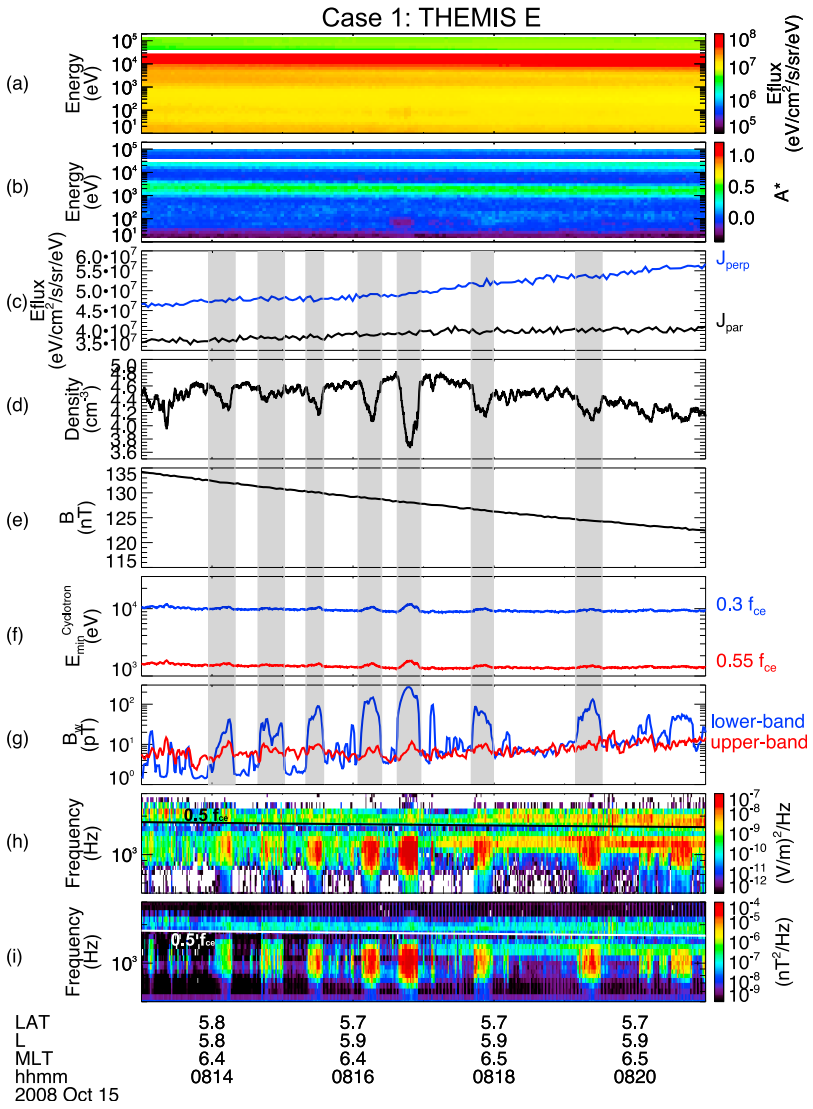


**Figure 1.** Case 1 observed by THEMIS E between 08:13 and 08:21 UT on 15 October 2008, when particle burst data was available. (a) Omnidirectional electron energy flux and (b) electron anisotropy ($A^*$) as functions of energy and time. (c) Electron energy flux over the energy of 3–30 keV roughly perpendicular (blue) and parallel (black) to the background magnetic field. (d) Total electron density inferred from the spacecraft potential, (e) total magnetic field, and (f) minimum resonant energy of electrons interacting with waves with normalized frequencies of 0.3 and 0.55 $f_{ce}$ through the first-order cyclotron resonance. (g) Integrated chorus wave amplitude over 0.05–0.5 $f_{ce}$ (lower band) and 0.5–0.8 $f_{ce}$ (upper band). Time-frequency spectrograms of (h) wave electric and (i) magnetic field spectral intensity. The solid lines in Figures 1h and 1i represent 0.5 $f_{ce}$.

(Figure 1g) exhibited substantial episodic intensification from a few pT to 300 pT. In contrast, the wave amplitude of the upper band chorus in the frequency band of 0.5–0.8 $f_{ce}$ remained weak (<20 pT). During this time interval, the omnidirectional electron energy fluxes were large (Figure 1a) and the electron anisotropy (Figure 1b) was elevated for electrons with energies of 1–5 keV and 10–30 keV. Figure 1c shows electron energy fluxes roughly perpendicular and parallel to the ambient magnetic field over the energy range 3–30 keV: the larger perpendicular flux provides a favorable condition for chorus excitation. The total electron density inferred from the spacecraft potential (Figure 1d) varied considerably, from ~3.7 to ~4.8 cm$^{-3}$, and the total magnetic field exhibited a monotonic decrease. The minimum energy of nonrelativistic electrons which undergo the first-order cyclotron resonance with parallel propagating chorus waves can be calculated by

$$E_{\min}^{\text{Cyclotron}} = \frac{B^2}{8\pi N}\frac{\Omega_e}{\omega}\left(1-\frac{\omega}{\Omega_e}\right)^3. \quad (1)$$

Here $N$ is the total electron density, $B$ is the ambient magnetic field, $\omega$ is the wave frequency, and $\Omega_e$ is the electron gyrofrequency. Figure 1f shows the minimum resonant energies of

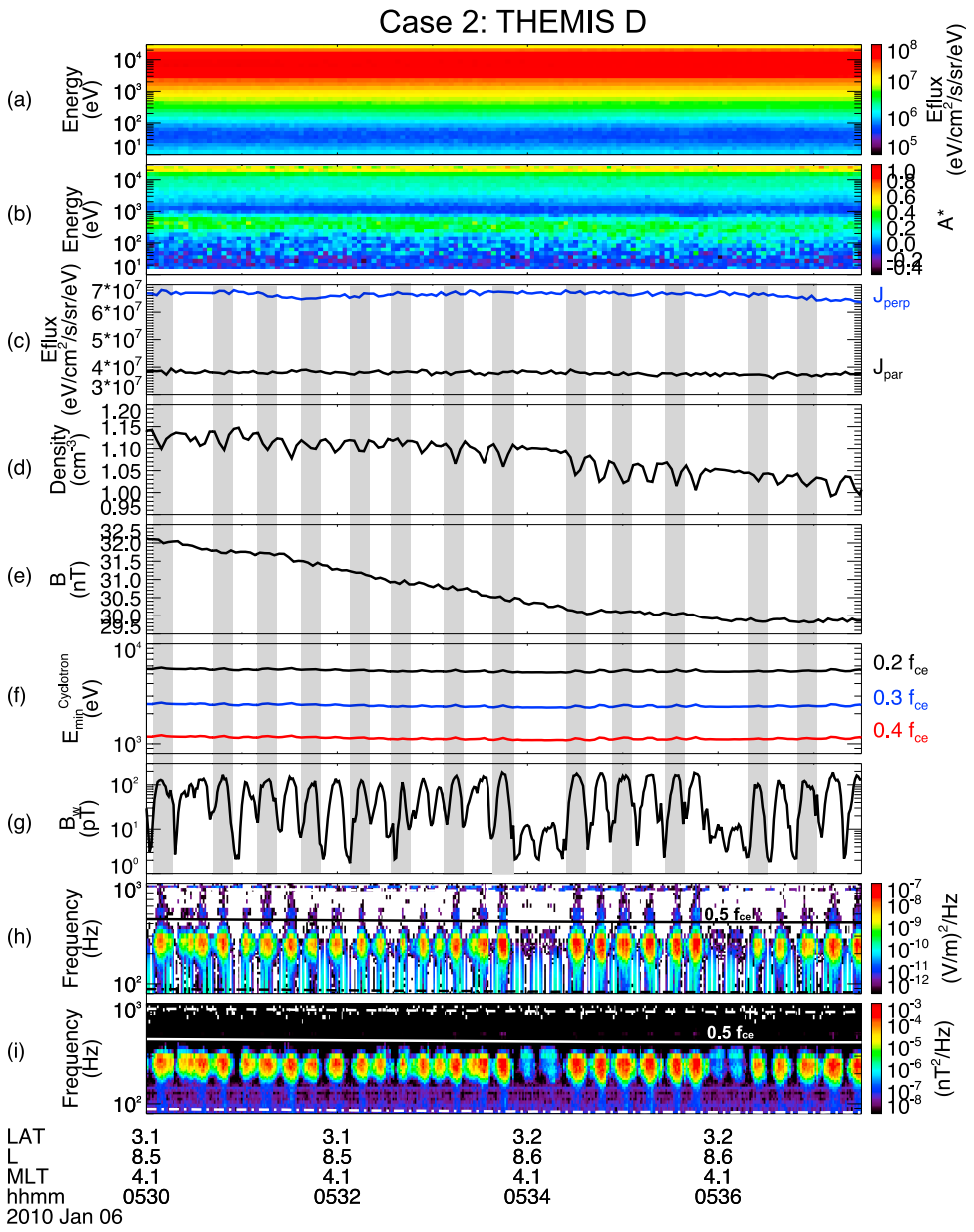


**Figure 2.** Similar parameters to Figure 1 but for Case 2 observed by THEMIS D during 05:30:00–05:37:30 UT. Minimum resonant energies of electrons are shown for wave frequencies of 0.2, 0.3, and 0.4 $f_{ce}$ in Figure 2f. Chorus wave amplitudes were integrated over 0.05–0.8 $f_{ce}$ and are shown in Figure 2g. Dashed, solid, and dashed-dotted lines indicate 1, 0.5, and 0.1 $f_{ce}$.

electrons for chorus waves with frequencies of 0.3 $f_{ce}$ and 0.55 $f_{ce}$, which show slight increase in response to the density depletions. Although the background magnetic field (Figure 1e) and resonant electron flux (Figure 1c) showed slight variations, a clear correlation with the wave amplitude modulation was not observed. We also analyzed electron flux data for each available energy channels from ESA (a few eV to ~30 keV) and SST (~25 keV to ~900 keV) to investigate the relevant energy of electrons which correlate with the total electron density change and found that none of the available electron energy channels showed the corresponding change. This suggests that the variations of total electron density are predominantly attributed to the variation in cold electrons (<a few eV), which are below the range of the ESA measurements. Most importantly, the lower band chorus wave amplitude increased when the electron density decreased and the wave amplitude was larger when the density was smaller, as highlighted by the light gray shading. Furthermore, the calculated correlation coefficient (not shown) between the total electron density and the lower band chorus wave amplitude (with zero time lag) is ~ −0.9, indicating that density depletions and wave amplitude enhancements are correlated remarkably well.

[9] Figure 2 shows similar lower band chorus intensification associated with density fluctuations observed by THEMIS D at ~4.1 MLT and a $L$ shell of ~8.5 on 6 January

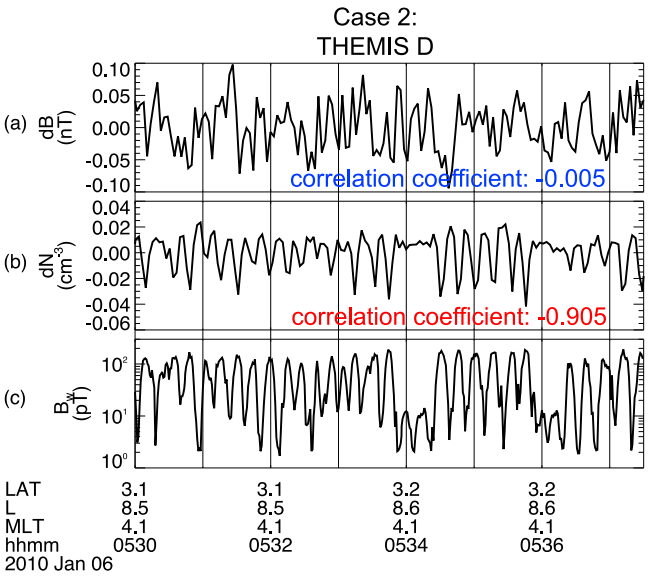


**Figure 3.** (a and b) The band-pass filtered total magnetic field and total electron density over 3–40 s. (c) Integrated chorus wave amplitude over 0.05–0.8 $f_{ce}$, the same as in Figure 2g.

2010. Over the interval of 05:30–05:38 UT, there were quasi-periodic intensifications of lower band chorus modulated over a period of 10–20 s (Figures 2h and 2i). Chorus magnetic field amplitude (Figure 2g) varied from a few pT to ~200 pT over intervals when the density (Figure 2d) was reduced. Over the entire interval, the electron energy flux (Figure 2a) remained large and the electron anisotropy ($A^*$) (Figure 2b) showed a modest value of ~0.4 in the energy range of ~100 eV–30 keV with a drop at ~1 keV. The perpendicular electron flux was larger than the parallel flux, thus providing favorable conditions for the chorus generation. The total electron density exhibited a modest (15%) variation during this time interval. We analyzed the electron flux data for each available energy channel from ESA and SST to investigate whether electrons in any specific energy range responded to the total electron density change and found that none of the available electron energy channels showed a corresponding change. Although the background magnetic field (Figure 2e) and resonant electron flux (Figure 2c) showed slight variations, they are not correlated with the chorus modulation. The minimum resonant energy for waves with frequencies of 0.2, 0.3, and 0.4 $f_{ce}$ (Figure 2f) changed slightly in response to the small variation in the total electron density. However, the chorus modulation is clearly associated with the variation in the total electron density.

[10] To quantify the correlation of the chorus wave amplitude with the variations in the total electron density and the background magnetic field, we band-pass filtered the data of the total electron density and the background magnetic field over 3–40 s. The resulting variations in the magnetic field and density are shown in Figures 3a and 3b and compared in Figure 3c to the integrated wave amplitude (same as Figure 2g). The calculated correlation coefficients are −0.005 between the filtered magnetic field and chorus wave amplitude and −0.905 between the filtered electron density and wave amplitude, indicating that depletions in density and increases in chorus wave amplitude have an almost one-to-one correlation, whereas the magnetic field perturbation is uncorrelated with the variation of the wave amplitude.

[11] In both Cases 1 and 2, wave spectrograms show quasi-periodically modulated chorus waves on a timescale ranging from a few to tens of seconds. Density depletions are correlated remarkably well with increases in the wave amplitude, such that in every density trough region, the maximum wave amplitude coincides almost exactly with the density minimum. On the other hand, electron fluxes in the measurable energy range on ESA and SST did not show a change corresponding to the total electron density, indicating that the energy of electrons responsible for the total density change is probably below a few eV.

### 2.2. Role of Density Enhancement in Chorus Modulation

[12] In this section, two typical DE events are shown, using the THEMIS particle burst data. Figure 4 shows similar parameters to Figure 1 but over the interval 12:52–12:59 UT on 27 November 2009 (Case 3), which occurred at a large $L$ shell of ~11.1 and at ~8.1 MLT. In Figures 4a and 4b, the electron flux was large at energy below ~10 keV with modest anisotropies, whereas the electron flux was very small at energy of 10–30 keV with large variations in anisotropies. The perpendicular electron flux was larger than the parallel flux, favorable for the chorus generation. Figure 4d shows three intervals of density enhancement at ~12:52:55, ~12:55:15, and ~12:57:30 UT (marked by gray shadings). These density enhancements appear to be related to increases in the energy flux of < 30 eV electrons, whose electron anisotropies ($A^*$) were negative, as shown in Figures 4a and 4b. The transient increases in the low energy electron flux are not due to photo electrons of spacecraft origin because the spacecraft potential decreased at these times. Spectrograms of wave electric and magnetic fields (Figures 4h and 4i) and the integrated wave magnetic amplitudes over 0.25–0.35 $f_{ce}$ and 0.35–0.45 $f_{ce}$ (Figure 4g) exhibited pronounced wave intensification associated with the three intervals of density enhancements. The resonant electron flux (Figure 4c) and background magnetic field (Figure 4e) showed no apparent variation in response to the wave amplitude. Interestingly, wave amplitudes (Figure 4g) increased substantially in association with these density enhancements, which also led to decreases in minimum resonant energy for both 0.3 and 0.4 $f_{ce}$. Moreover, the chorus amplitude was largest at the density peak and tended to be smaller as the density fell to background levels.

[13] Figure 5 shows an interval of pronounced chorus enhancements observed on 24 February 2010 by THEMIS D at ~5.0 MLT at a $L$ shell of ~7.8. This event (Case 4) shows much larger density enhancements than those in Case 3. In Figures 5a and 5b, the electron energy flux was large and the electron anisotropy ($A^*$) was positive at energies larger than ~1 keV. The perpendicular component of the resonant electron flux was larger than the parallel flux, as shown in Figure 5c. The total electron density (Figure 5d) varied substantially from 2 to 10 $cm^{-3}$, which was indeed associated with the corresponding variation in energy flux

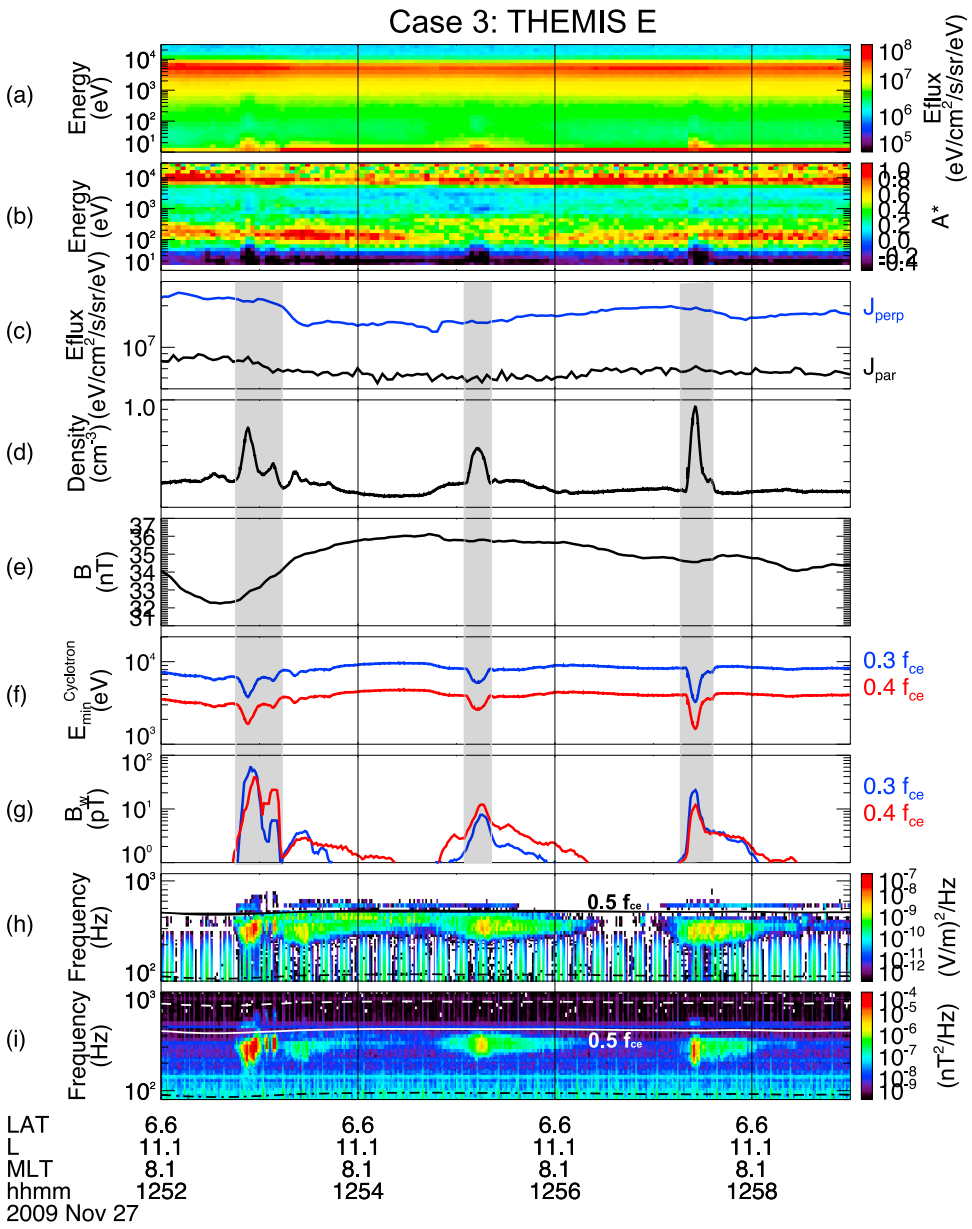


**Figure 4.** The same parameters as shown in Figure 1, but for Case 3 observed by THEMIS E during 12:52–12:59 UT. In Figure 4f the minimum resonant energies of electrons are shown for waves with frequencies of 0.3 and 0.4 $f_{ce}$. Chorus wave amplitudes were integrated over 0.25–0.35 $f_{ce}$ (blue) and 0.35–0.45 $f_{ce}$ (red) and are shown in Figure 4g.

for low energy electrons (<~500 eV), whose anisotropies were negative. The intensity of the background magnetic field (Figure 5e) gradually increased from higher to lower $L$ shells without showing corresponding variations in the wave amplitudes. Significant variations in the minimum resonant energy due to the substantial change in the total electron density are shown in Figure 5f for various wave frequencies. In Figures 5h and 5i wave electric and magnetic fields of lower band chorus varied significantly in both the intensity and the frequencies of the chorus waves. The wave magnetic field intensity in Figure 5i was integrated over a frequency range 0.05–0.5 $f_{ce}$ and is shown in Figure 5g. The comparison of the total electron density and the chorus wave amplitude shows that the wave amplitude increased and the central frequency of the generated waves decreased, when the total electron density increased (and vice versa).

[14] For a fixed minimum resonant energy of electrons, the resonant wave frequency can be calculated using equation (1). An increase in the total electron density would allow waves with lower frequencies to resonate with the electron population with a given energy, which contains a source of free energy for the wave generation. We calculated the corresponding wave frequency for electrons with a minimum resonant energy of ~8 keV, which is an important population for chorus generation with both large fluxes and sufficient anisotropies ($A$*). Figures 6a and 6b show the

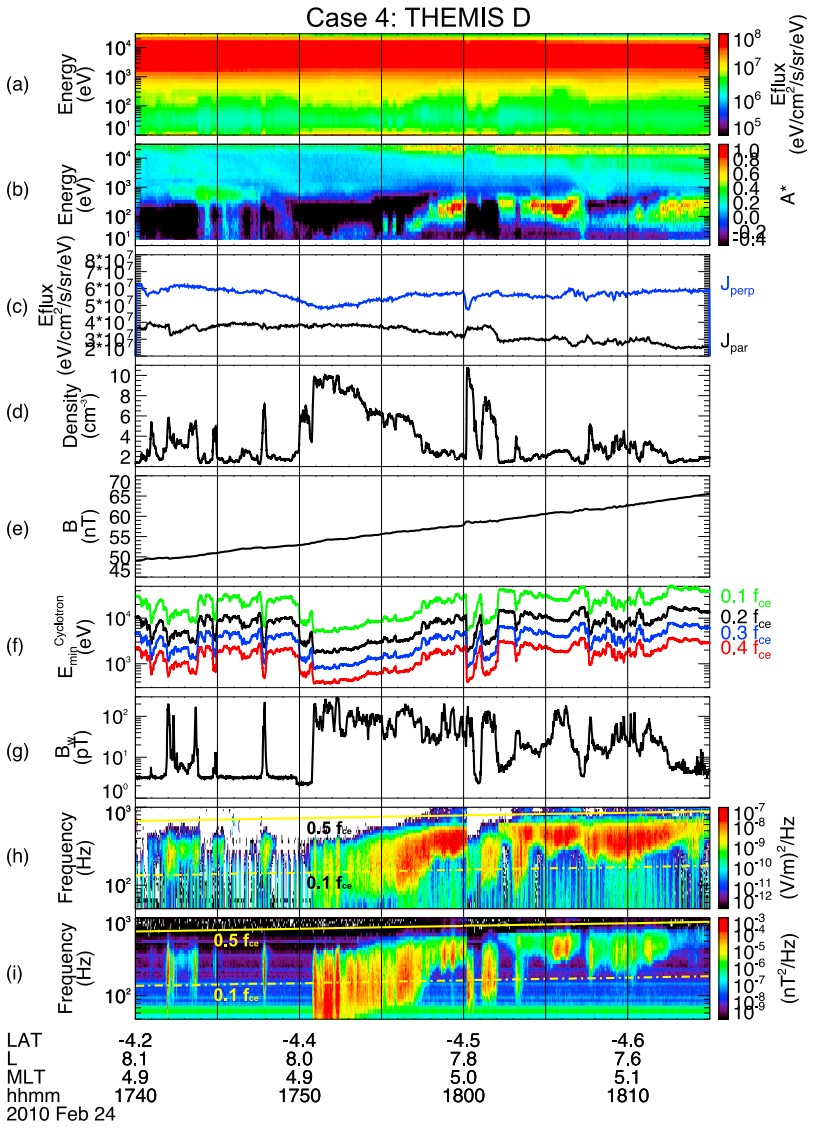


**Figure 5.** The same parameters as shown in Figure 1, but for Case 4 observed by THEMIS D during 17:40–18:15 UT. Figure 5f shows minimum resonant energies of electrons for wave frequencies of 0.1, 0.2, 0.3, and 0.4 $f_{ce}$. Chorus wave amplitudes were integrated over 0.05–0.8 $f_{ce}$ and are shown in Figure 5g.

total electron density and time-frequency spectrograms of wave magnetic field intensity in Case 4 during the same period as in Figure 5. The solid white line in Figure 6b represents the calculated resonant wave frequency for electrons with the minimum resonant energy of 8 keV. The predicted resonant wave frequency agrees remarkably well with the observed central wave frequency. This consistency confirms that generated wave frequencies tend to be smaller when the total electron density increases (and vice versa).

[15] In both Cases 3 and 4, wave spectrograms show modulating chorus waves on a timescale from a few seconds to tens of seconds. In both events, density enhancements are well correlated with increases in the wave amplitude, such that near the density crest, the maximum of the wave intensity coincides almost precisely with the density peak. Chorus waves relevant to DE events are not likely to be quasi-periodic but rather irregular emissions. In addition, low energy electron fluxes (<a few hundred eV) show the corresponding enhancements with respect to the density enhancements.

### 2.3. Global Distributions of DD and DE Events

[16] The case analyses of both DD and DE events shown above indicate that chorus wave amplitudes increase in association with both density depletions and enhancements. In order to comprehensively investigate conditions and locations where density depletions and enhancements play a significant role in chorus intensity enhancement, we systematically surveyed all of the particle burst data available between 1 June 2008 and 1 August 2010 in regions with $L$ shells between 5 and 12, observed by the three inner probes of THEMIS A, D, and E.

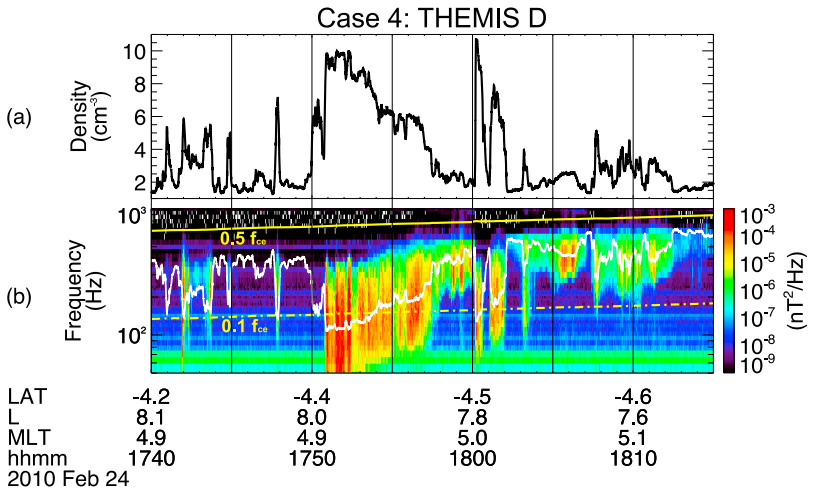


**Figure 6.** (a) Total electron density and (b) time-frequency spectrograms of wave magnetic field intensity in Case 4. In Figure 6b, the two yellow lines represent 0.5 (solid) and 0.1 $f_{ce}$ (dashed-dotted) and solid white line represents the calculated resonant wave frequency for electrons with energy of ~8 keV.

[17] Events have been analyzed using integrated wave amplitudes over 0.05–0.8 $f_{ce}$ and total electron density. We calculated the correlation coefficients of the total electron density and the wave amplitude ($CC_{nbw}$) every 1 min and recorded the maximum wave amplitude during each 1 min interval, and $L$ shell and MLT at the center time of the 1 min interval. The selected events were required to satisfy the following criteria. First, the maximum wave amplitude of chorus waves during a 1 min time interval exceeds 20 pT in order to select reasonably intense chorus events. Second, for DE events $CC_{nbw}$ is larger than 0.8, whereas for DD events $CC_{nbw}$ is smaller than −0.8. Third, events must occur outside the plasmapause but inside the magnetopause. Note that the location of the plasmapause is determined using the method described by *Li et al.* [2010b]. Finally, events must occur in the dominant chorus region between 22 and 14 MLT in order to exclude hiss in plumes, which predominantly occurs in the late afternoon and dusk sectors [*Meredith et al.*, 2004].

[18] Figure 7a shows the global distribution of number of samples from all available particle burst data from 1 June 2008 to 1 August 2010 sorted into bins of 1 L × 1 MLT in the regions between 5 and 12 $R_E$ and from 22 to 14 MLT. Figures 7b and 7c show the distribution of DE and DD events respectively. The majority of DE events occur between the dawn and afternoon sector, whereas most DD events are distributed from the premidnight to the dawn sector. On the nightside (22–03 MLT), both DD and DE events mostly occur at $L$ shells less than 8, while extending to up to ~12 $R_E$ on the dayside. In the dawn sector both DE and DD events occur between 6 and 12 $R_E$.

[19] By systematically investigating the statistical distribution of DD and DE events as well as the detailed case studies, we found notable differences in the two classes of chorus modulation. First, quasi-periodic chorus modulations are more likely to be associated with density depletions, while events associated with density enhancements are likely to occur with an irregular time period. This may suggest that the quasi-periodically-occurring pulsating aurora is probably more relevant to the DD events. Second, DE events predominantly occur on the dayside, while DD events occur more commonly from the premidnight to the

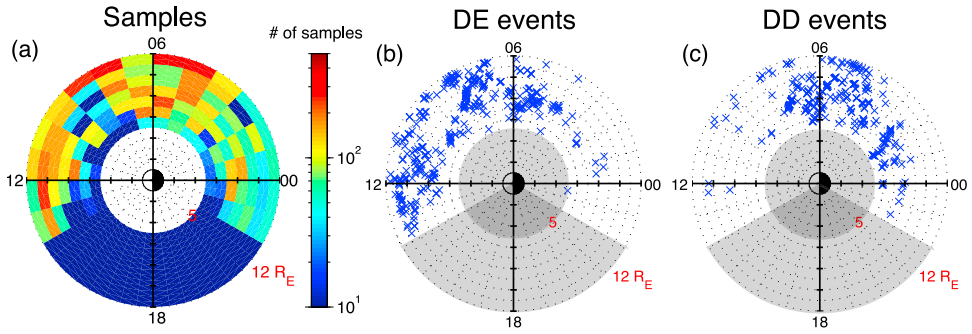


**Figure 7.** Global distributions of (a) number of samples from all available particle burst data sorted into bins of 1 $L$ × 1 MLT (b) DE events and (c) DD events in the dominant chorus source region between 5 and 12 $R_E$ and from 22 to 14 MLT. The gray shaded regions in Figures 7b and 7c represent the area, where this statistical survey is excluded.

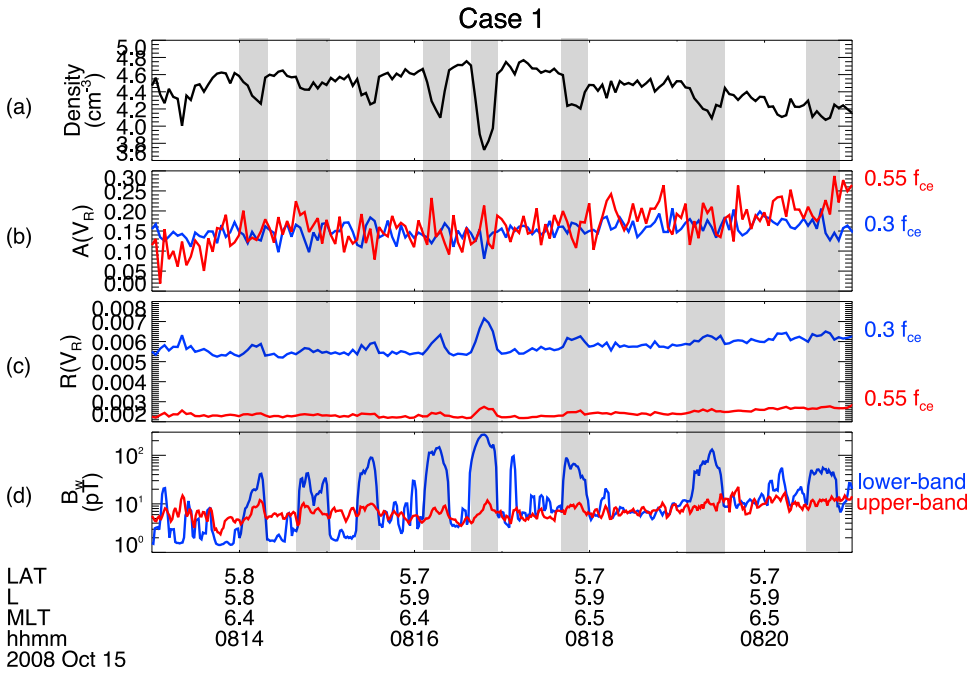


**Figure 8.** Parameters in Case 1 during the same period as in Figure 1. (a) Total electron density, (b) electron anisotropy $A(V_R)$ and (c) ratio of resonant electrons over total electrons $R(V_R)$ for wave frequencies of 0.3 and 0.55 $f_{ce}$. (d) Integrated chorus wave amplitudes for the lower band (0.05–0.5 $f_{ce}$) and upper band (0.5–0.8 $f_{ce}$) indicated by blue and red lines respectively.

dawn sector among the events surveyed from 22 to 14 MLT. Third, electron fluxes for low energies (<a few hundred eV) increase in response to the density enhancements in DE events, but no corresponding electron flux variation is identified for density decreases in the measurable energy channels of both ESA and SST in DD events. This implies that changes in the electron population in DD events likely occur for very cold electrons (<~5 eV), which cannot be measured by the ESA instrument.

## 3. Calculation of Linear Growth Rates

[20] The above observational results showed that both depletions and enhancements in density can lead to the amplification of chorus wave intensity. In this section, we evaluate two parameters which contribute to the linear growth rates of whistler mode waves based on observations and investigate how well linear growth rates are able to explain the observed wave modulation for both DD and DE events. The calculation of linear growth rates has been performed using the method described in detail by *Li et al.* [2011].

[21] We select Case 1 (DD) and Case 3 (DE) to calculate the linear growth rates and compare with observed wave amplitudes. Figures 8a and 8d show the total electron density and integrated wave amplitudes over 0.05–0.5 $f_{ce}$ (lower band) and 0.5–0.8 $f_{ce}$ (upper band) in Case 1, same as in Figures 1d and 1g. Lower band chorus wave amplitudes varied substantially from a few pT to ~300 pT, whereas the amplitude of the upper band chorus was much weaker (<20 pT). The two factors contributing to the linear growth rates, the electron anisotropy for a fixed resonant energy $A(V_R)$ and the ratio of resonant electrons to total electrons $R(V_R)$, are shown for wave frequencies of 0.3 and 0.55 $f_{ce}$ in Figures 8b and 8c respectively. $R(V_R)$ increased (particularly for 0.3 $f_{ce}$) when the total density decreased, thus causing an increase in the linear growth rates. In contrast, the variation in $A(V_R)$ was not correlated with the observed wave amplitude. $A(V_R)$ for 0.55 $f_{ce}$ was comparable to that for 0.3 $f_{ce}$, although the generation of chorus waves at 0.55 $f_{ce}$ requires larger $A(V_R)$ for the same growth rate. This may explain the fact that the upper band chorus was significantly weaker than the lower band chorus observed by THEMIS E. The modest change in $R(V_R)$ compared to the two order of magnitude enhancement in wave amplitudes suggests that the magnetospheric plasma was in a state close to marginal stability [*Kennel and Petschek*, 1966], which allowed small increases in the linear growth rates to drive rapid wave amplification. In summary, density depletions in Case 1 cause the increase in $R(V_R)$, thus contributing to the increase in the linear growth rates.

[22] Figure 9 shows similar parameters as in Figure 8 but for Case 3 (DE). In Case 3, the increase in the wave amplitude was associated with the density enhancements, in contrast to Case 1. The three main density enhancements in Figure 9a were associated with a corresponding increases in $R(V_R)$. Although $A(V_R)$ was associated with slight variations at 0.4 $f_{ce}$, it was not well correlated with the observed wave amplitude. At 0.3 $f_{ce}$ $A(V_R)$ showed substantial fluctuations probably due to the larger uncertainty caused by low electron fluxes at > ~10 keV shown in Figures 4a and 4b. In summary, density enhancements in Case 3 account for the increases in $R(V_R)$, thus contributing to the increase in the linear growth rates.

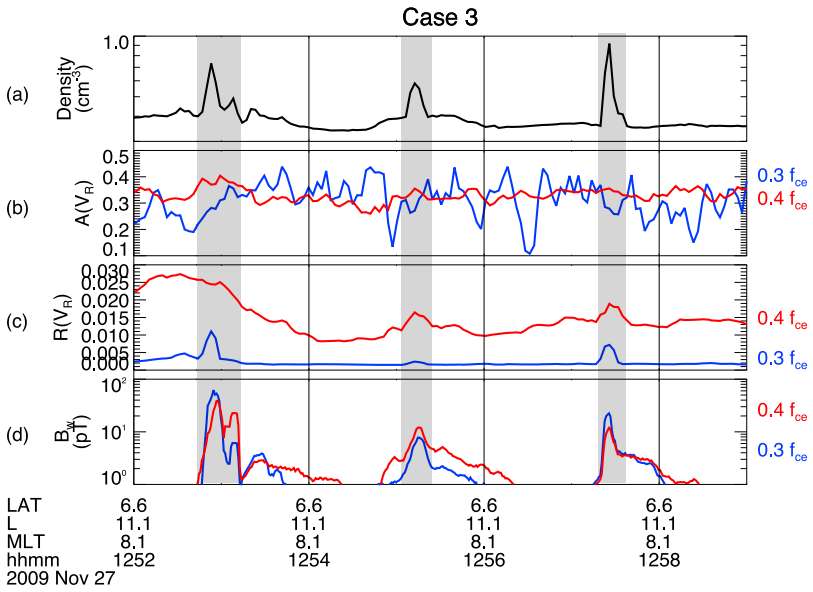


**Figure 9.** Parameters in Case 3 during the same period as in Figure 4. (a) Total electron density, (b) $A(V_R)$ and (c) $R(V_R)$ for wave frequencies of 0.3 and 0.4 $f_{ce}$. (d) Integrated chorus wave amplitude over 0.25–0.35 (blue) and 0.35–0.45 $f_{ce}$ (red).

[23] Calculations of linear growth rates in DD and DE events in Case 1 and 3 showed that both density depletions and enhancements can lead to an increase in $R(V_R)$ without showing corresponding significant changes in $A(V_R)$, thus increasing the overall linear growth rates. $R(V_R)$ can roughly be interpreted as the fraction of resonant electrons to total electrons. The total electron density can affect both the numerator and the denominator of $R(V_R)$. An increase in the total electron density reduces the minimum energy (from equation (1)) of energetic resonant electrons, which results in a larger density of resonant electrons, thus increasing the numerator of $R(V_R)$. On the other hand, a decrease in the total electron density can also directly increase $R(V_R)$ by reducing the denominator of $R(V_R)$. Therefore, the overall change in $R(V_R)$ is determined by whether the numerator or the denominator dominates in the ratio variation. Consequently, both increases and decreases in density can cause increases in linear growth rates, and thus resulting in the amplification of the wave intensity.

## 4. Discussion

[24] Using measured parameters from THEMIS, we evaluated the evolution of electron anisotropy $A(V_R)$ and the fractional density of resonant electrons $R(V_R)$, which contribute to the linear growth rates of chorus waves and compared the results with the observed wave amplitudes for Case 1 and Case 3. In both DD and DE events, the variations in $R(V_R)$ are roughly consistent with the changes of observed wave amplitudes, whereas $A(V_R)$ does not show clear corresponding variations but is close to the marginal stability. Linear growth is important for small amplitude chorus and also plays a dominant role in the early stage of wave generation for strong chorus waves [e.g., *Devine et al.*, 1995; *Omura et al.*, 2008]. Furthermore, linear growth rates provide essential information on whether the plasma conditions exceed the marginal stability criterion and thus allow waves to grow to the observable level. The onset of instability may be triggered primarily by variations in total electron density of a marginally stable plasma. Substantial changes (more than a factor of 10) in observed wave intensity variations (Figure 9d) and relatively smaller variations (~50%) in calculated fluctuations in linear growth rates (Figure 9c) are not unreasonable under such conditions, since small changes in linear growth rates can lead to large changes in wave amplitudes. However, whether the difference in linear growth rates is sufficient to explain the observed modulating wave intensity requires consideration of nonlinear and wave propagation effects. Nonlinear wave growth tends to play an important role after the linear growth phase particularly for the large amplitude waves, by rapidly increasing the wave amplitude prior to saturation [e.g., *Nunn et al.*, 1997; *Omura and Summers*, 2004; *Omura et al.*, 2008]. Although linear theory supports our hypothesis of modulation of chorus wave intensity by both density enhancements and depletions, other mechanisms of density modulated chorus waves should also be considered. The modulated wave intensity associated with density variations may be a consequence of propagation through the region with density fluctuations [*Smith*, 1961; *Angerami*, 1970; *Gorney and Thorne*, 1980; *Streltsov et al.*, 2006]. Therefore, it is important to understand whether the observed variations in density are sufficient to trap the chorus waves in either density crests or troughs. However, the evaluation of wave propagation characteristics in the region of density crests and troughs is beyond the scope of the present study and is left for further investigation.

[25] Pulsating aurora, blinking on and off on a timescale from ~1 s to tens of seconds in the upper atmosphere, is known to be generated primarily by precipitating energetic electrons (>10 keV) [e.g., *Smith et al.*, 1980; *Davidson*,

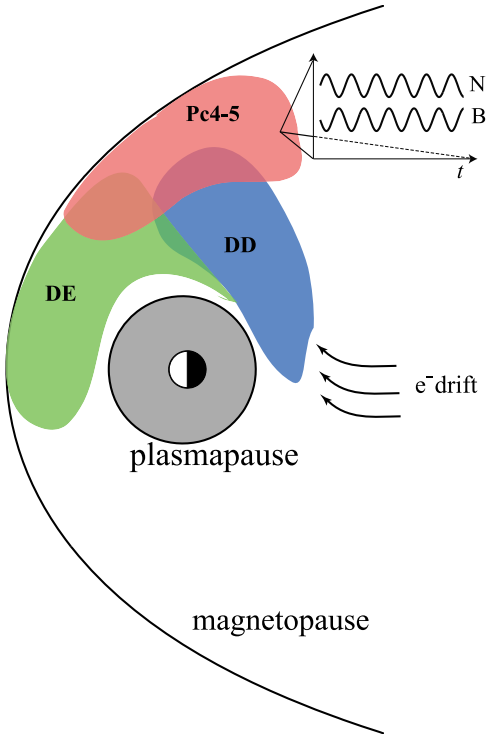


**Figure 10.** A schematic illustration showing the global distribution of chorus modulation associated with three different mechanisms in the equatorial magnetosphere. The black arrows represent trajectories of electrons injected from the plasma sheet near the midnight sector and the gray region indicates high-density plasmasphere. Red, blue and green regions represent chorus modulation relevant to compressional Pc4–5 pulsations with an anti–correlation between the density and the magnetic field (shown next to the red region), density depletions (DD), and density enhancements (DE) respectively.

1990]. Previous studies showed that chorus is the driver of the pulsating aurora through scattering plasma sheet electrons [e.g., *Johnstone*, 1978, 1983; *Davidson*, 1990; *Miyoshi et al.*, 2010; *Nishimura et al.*, 2010]. Pulsating aurora typically occurs from the premidnight to the dawn sector with a higher occurrence in the dawn sector after 4 MLT and the pulsating aurora regions tend to be higher in latitude in the dawn sector than at midnight [e.g., *Oguti et al.*, 1981]. Our study shows that the modulation of chorus waves, which leads to the modulation of the auroral luminosity, can be caused by density variations. DD events are predominantly located from the premidnight to the dawn sector at lower $L$ shells at midnight and higher $L$ shells in the dawn sector. Since the preferential region of DD events agrees well with the dominant region of pulsating aurora and DD events are frequently associated with quasi-periodically modulated chorus waves, we suggest that density depletions may play an important role in modulating chorus wave intensity and thus may be responsible for driving the pulsating aurora.

[26] Figure 10 presents a schematic illustration of the dominant region where chorus modulation by various mechanisms occur, discussed in both the companion paper of *Li et al.* [2011] and the present paper. Chorus waves are generated by anisotropic electrons injected from the plasma sheet [*Burtis and Helliwell*, 1969; *Tsurutani and Smith*, 1974]. In the absence of fresh electron injection events, the suprathermal population of electrons in the region exterior to the plasmapause appears to approach a state of marginal stability [e.g., *Kennel and Petschek*, 1966]. On the other hand, statistical results on the averaged electron anisotropy in the energy range between a few hundred eV and ~100 keV show positive values in the chorus dominant region [*Li et al.*, 2010a]. As these electrons (indicated by black arrows) drift from the midnight through the dawn toward the noon sector, where plasma conditions are close to the marginal stability with a positive anisotropy the onset of wave instability can be triggered by a change in the background plasma parameters. Between midnight and dawn, density depletions have a remarkably good correlation with the intensification of chorus waves. DD events mainly occur at $L$ shells of 5–8 in the midnight sector, and extend to higher $L$ shells in the dawn sector. DD events are more likely to be associated with quasi-periodically modulated chorus and may be related to the generation of pulsating aurora. In the dawnside (3–8 MLT) outer magnetosphere ($L > 8$), compressional Pc4–5 pulsations with an anticorrelation between the density and the magnetic field play an important role in modulating chorus waves on a timescale of tens of seconds to a few minutes. Although previous studies showed that compressional Pc4–5 pulsations are commonly observed in both the dusk and dawn sectors at $L > 8$ at low geomagnetic latitudes [e.g., *Takahashi et al.*, 1990; *Zhu and Kivelson*, 1991], chorus modulation by compressional Pc4–5 pulsations predominantly occurs in the dawn sector, probably due to insufficient resonant electron fluxes in the dusk sector [e.g., *Bortnik and Thorne*, 2007; *Li et al.*, 2010a]. Between dawn and noon, modulation of chorus by density enhancements predominates at $L$ shells extending from outside the plasmapause up to the magnetopause. Density enhancements also tend to reduce the central frequency of the generated chorus waves and vice versa. In summary, when plasma conditions are close to marginal stability, chorus modulation at various locations is caused by predominantly different changes in the plasma parameters.

## 5. Summary and Conclusions

[27] We have investigated the relationship between density variations and chorus wave intensity using THEMIS data in the near–equatorial magnetosphere. Using linear theory we have also evaluated the role of density variations in growth rates of chorus waves. The principal conclusions in this study can be summarized as follows.

[28] 1. In a state of marginal stability for suprathermal electrons responsible for chorus generation, modulation of chorus wave intensity is frequently associated with density variations on a timescale from a few seconds to tens of seconds, which overlaps with typical timescales of pulsating aurora.

[29] 2. Density depletions are correlated remarkably well with increases in chorus wave amplitude. The smallest values of the total electron density correlate with the most significant increases in wave amplitude.

[30] 3. Density enhancements lead to the amplification of the chorus wave intensity, thus correlating very well with

modulated chorus wave amplitudes. Density enhancements also tend to reduce the central frequency of the generated chorus waves and vice versa.

[31] 4. Statistical results show that DD events predominantly occur from premidnight to dawn, whereas DE events commonly occur between dawn and afternoon among the events surveyed from 22 to 14 MLT. DD events are confined to $L < 8$ on the nightside and DE events extend to higher $L$ shells up to 12 on the dayside. DD events are more likely to be relevant to the quasi-periodic chorus and may be related to the generation of the pulsating aurora.

[32] 5. Both density depletions and enhancements can lead to the increase in linear growth rates of chorus waves. However, other potential mechanisms such as chorus wave trapping in density crests and troughs cannot be excluded.

[33] **Acknowledgments.** This research was funded by the NSF grants AGS-0840178 and ATM-0802843, NASA Heliophysics Theory Program grant NNX08A135G, and NASA NAS5–02099. The authors acknowledge A. Roux and O. Le Contel for use of SCM data; J. W. Bonnell and F. S. Mozer for use of EFI data; C. W. Carlson and J. P. McFadden for use of ESA data; D. Larson and R. P. Lin for use of SST data; and K. H. Glassmeier, U. Auster, and W. Baumjohann for the use of FGM data provided under the lead of the Technical University of Braunschweig and with financial support through the German Ministry for Economy and Technology and the German Center for Aviation and Space (DLR) under contract 50 OC 0302.

[34] Robert Lysak thanks Nigel Meredith and another reviewer for their assistance in evaluating this paper.

## References

Angerami, J. J. (1970), Whistler duct properties deduced from VLF observations made with the Ogo 3 satellite near the magnetic equator, *J. Geophys. Res.*, *75*, 6115–6135, doi:10.1029/JA075i031p06115.

Bortnik, J., and R. M. Thorne (2007), The dual role of ELF/VLF chorus waves in the acceleration and precipitation of radiation belt electrons, *J. Atmos. Sol. Terr. Phys.*, *69*, 378–386, doi:10.1016/j.jastp.2006.05.030.

Burtis, W. J., and R. A. Helliwell (1969), Banded chorus—A new type of VLF radiation observed in the magnetosphere by OGO 1 and OGO 3, *J. Geophys. Res.*, *74*, 3002–3010, doi:10.1029/JA074i011p03002.

Chen, Y., G. D. Reeves, and R. H. W. Friedel (2007), The energization of relativistic electrons in the outer Van Allen radiation belt, *Nat. Phys.*, *3*, 614–617, doi:10.1038/nphys655.

Coroniti, F. V., and C. F. Kennel (1970), Electron precipitation pulsations, *J. Geophys. Res.*, *75*, 1279–1289, doi:10.1029/JA075i007p01279.

Davidson, G. T. (1979), Self-modulated VLF wave-electron interactions in the magnetosphere: A cause of auroral pulsations, *J. Geophys. Res.*, *84*, 6517–6523, doi:10.1029/JA084iA11p06517.

Davidson, G. T. (1990), Pitch-angle diffusion and the origin of temporal and spatial structures in morningside aurorae, *Space Sci. Rev.*, *53*, 45–82, doi:10.1007/BF00217428.

Devine, P. E., S. C. Chapman, and J. W. Eastwood (1995), One- and two-dimensional simulations of whistler mode waves in an anisotropic plasma, *J. Geophys. Res.*, *100*, 17,189–17,203, doi:10.1029/95JA00842.

Gorney, D. J., and R. M. Thorne (1980), A comparative ray-trace study of whistler ducting processes in the Earth's plasmasphere, *Geophys. Res. Lett.*, *7*, 133–136, doi:10.1029/GL007i002p00133.

Helliwell, R. A. (1967), A theory of discrete emissions from the magnetosphere, *J. Geophys. Res.*, *72*, 4773–4790, doi:10.1029/JZ072i019p04773.

Horne, R. B., and R. M. Thorne (1998), Potential waves for relativistic electron scattering and stochastic acceleration during magnetic storms, *Geophys. Res. Lett.*, *25*, 3011–3014, doi:10.1029/98GL01002.

Horne, R. B., R. M. Thorne, N. P. Meredith, and R. R. Anderson (2003), Diffuse auroral electron scattering by electron cyclotron harmonic and whistler mode waves during an isolated substorm, *J. Geophys. Res.*, *108*(A7), 1290, doi:10.1029/2002JA009736.

Horne, R. B., R. M. Thorne, S. A. Glauert, J. M. Albert, N. P. Meredith, and R. R. Anderson (2005a), Timescale for radiation belt electron acceleration by whistler mode chorus waves, *J. Geophys. Res.*, *110*, A03225, doi:10.1029/2004JA010811.

Horne, R. B., et al. (2005b), Wave acceleration of electrons in the Van Allen radiation belts, *Nature*, *437*, 227–230, doi:10.1038/nature03939.

Huang, G.-L., D.-Y. Wang, and Q.-W. Song (2004), Whistler waves in Freja observations, *J. Geophys. Res.*, *109*, A02307, doi:10.1029/2003JA010137.

Johnstone, A. D. (1978), Pulsating aurora, *Nature*, *274*, 119–126, doi:10.1038/274119a0.

Johnstone, A. D. (1983), The mechanism of pulsating aurora, *Ann. Geophys.*, *1*, 397–410.

Kennel, C. F., and H. E. Petschek (1966), Limit on stable trapped particle fluxes, *J. Geophys. Res.*, *71*, 1–28.

Koons, H. C. (1989), Observations of large-amplitude, whistler mode wave ducts in the outer plasmasphere, *J. Geophys. Res.*, *94*, 15,393–15,397.

Lepine, D. R., D. A. Bryant, and D. S. Hall (1980), A 2.2-Hz modulation of auroral electrons imposed at the geomagnetic equator, *Nature*, *286*, 469–471, doi:10.1038/286469a0.

Li, W., Y. Y. Shprits, and R. M. Thorne (2007), Dynamic evolution of energetic outer zone electrons due to wave-particle interactions during storms, *J. Geophys. Res.*, *112*, A10220, doi:10.1029/2007JA012368.

Li, W., R. M. Thorne, V. Angelopoulos, J. Bortnik, C. M. Cully, B. Ni, O. LeContel, A. Roux, U. Auster, and W. Magnes (2009), Global distribution of whistler-mode chorus waves observed on the THEMIS spacecraft, *Geophys. Res. Lett.*, *36*, L09104, doi:10.1029/2009GL037595.

Li, W., et al. (2010a), THEMIS analysis of observed equatorial electron distributions responsible for the chorus excitation, *J. Geophys. Res.*, *115*, A00F11, doi:10.1029/2009JA014845.

Li, W., R. Thorne, J. Bortnik, Y. Nis himura, V. Angelopoulos, L. Chen, J. P. McFadden, and J. W. Bonnell (2010b), Global distributions of suprathermal electrons observed on THEMIS and potential mechanisms for access into the plasmasphere, *J. Geophys. Res.*, *115*, A00J10, doi:10.1029/2010JA015687.

Li, W., R. M. Thorne, J. Bortnik, Y. Nishimura, and V. Angelopoulos (2011), Modulation of whistler mode chorus waves: 1. Role of compressional Pc4–5 pulsations, *J. Geophys. Res.*, *116*, A06205, doi:10.1029/2010JA016312.

Lorentzen, K. R., J. B. Blake, U. S. Inan, and J. Bortnik (2001), Observations of relativistic electron microbursts in association with VLF chorus, *J. Geophys. Res.*, *106*, 6017–6027, doi:10.1029/2000JA003018.

Meredith, N. P., R. B. Horne, and R. R. Anderson (2001), Substorm dependence of chorus amplitudes: Implications for the acceleration of electrons to relativistic energies, *J. Geophys. Res.*, *106*, 13,165–13,178, doi:10.1029/2000JA900156.

Meredith, N. P., R. B. Horne, R. H. A. Iles, R. M. Thorne, D. Heynderickx, and R. R. Anderson (2002), Outer zone relativistic electron acceleration associated with substorm-enhanced whistler mode chorus, *J. Geophys. Res.*, *107*(A7), 1144, doi:10.1029/2001JA900146.

Meredith, N. P., R. B. Horne, R. M. Thorne, and R. R. Anderson (2003), Favored regions for chorus-driven electron acceleration to relativistic energies in the Earth's outer radiation belt, *Geophys. Res. Lett.*, *30*(16), 1871, doi:10.1029/2003GL017698.

Meredith, N. P., R. B. Horne, R. M. Thorne, D. Summers, and R. R. Anderson (2004), Substorm dependence of plasmaspheric hiss, *J. Geophys. Res.*, *109*, A06209, doi:10.1029/2004JA010387.

Miyoshi, Y., Y. Katoh, T. Nishiyama, T. Sakanoi, K. Asamura, and M. Hirahara (2010), Time of flight analysis of pulsating aurora electrons, considering wave-particle interactions with propagating whistler mode waves, *J. Geophys. Res.*, *115*, A10312, doi:10.1029/2009JA015127.

Moullard, O., A. Masson, H. Laakso, M. Parrot, P. Décréau, O. Santolik, and M. Andre (2002), Density modulated whistler mode emissions observed near the plasmapause, *Geophys. Res. Lett.*, *29*(20), 1975, doi:10.1029/2002GL015101.

Ni, B., R. M. Thorne, Y. Y. Shprits, and J. Bortnik (2008), Resonant scattering of plasma sheet electrons by whistler-mode chorus: Contribution to diffuse auroral precipitation, *Geophys. Res. Lett.*, *35*, L11106, doi:10.1029/2008GL034032.

Nishimura, Y., et al. (2010), Identifying the driver of pulsating aurora, *Science*, *330*(6000), 81–84, doi:10.1126/science.1193186.

Nunn, D., Y. Omura, H. Matsumoto, I. Nagano, and S. Yagitani (1997), The numerical simulation of VLF chorus and discrete emissions observed on the Geotail satellite using a Vlasov code, *J. Geophys. Res.*, *102*, 27,083–27,097, doi:10.1029/97JA02518.

O'Brien, T. P., M. D. Looper, and J. B. Blake (2004), Quantification of relativistic electron microburst losses during the GEM storms, *Geophys. Res. Lett.*, *31*, L04802, doi:10.1029/2003GL018621.

Oguti, T., S. Kokubun, K. Hayashi, K. Tsuruda, S. Machida, T. Kitamura, O. Saka, and T. Watanabe (1981), Statistics of pulsating aurora on the basis of all-sky TV data from five stations. 1. Occurrence frequency, *Can. J. Phys.*, *59*, 1150–1157, doi:10.1139/p81-152.

Omura, Y., and D. Summers (2004), Computer simulations of relativistic whistler-mode wave-particle interactions, *Phys. Plasmas*, *11*, 3530, doi:10.1063/1.1757457.

Omura, Y., Y. Katoh, and D. Summers (2008), Theory and simulation of the generation of whistler-mode chorus, *J. Geophys. Res.*, *113*, A04223, doi:10.1029/2007JA012622.

Pasmanik, D. L., E. E. Titova, A. G. Demekhov, V. Trakhtengerts, O. Santolik, F. Jiricek, K. Kudela, and M. Parrot (2004), Quasi-periodic ELF/VLF wave emissions in the Earth's magnetosphere: Comparison of satellite observations and modeling, *Ann. Geophys.*, *22*, 4351–4361, doi:10.5194/angeo-22-4351-2004.

Sazhin, S. S., and M. Hayakawa (1992), Magnetospheric chorus emissions: A review, *Planet. Space Sci.*, *40*, 681–697, doi:10.1016/0032-0633(92)90009-D.

Sazhin, S. S., and M. Hayakawa (1994), Periodic and quasiperiodic VLF emissions, *J. Atmos. Terr. Phys.*, *56*, 735–753, doi:10.1016/0021-9169(94)90130-9.

Scarf, F. L., and C. R. Chappell (1973), An association of magnetospheric whistler dispersion characteristics with changes in local plasma density, *J. Geophys. Res.*, *78*, 1597–1602, doi:10.1029/JA078i010p01597.

Shprits, Y. Y., R. M. Thorne, R. B. Horne, S. A. Glauert, M. Cartwright, C. T. Russell, D. N. Baker, and S. G. Kanekal (2006), Acceleration mechanism responsible for the formation of the new radiation belt during the 2003 Halloween solar storm, *Geophys. Res. Lett.*, *33*, L05104, doi:10.1029/2005GL024256.

Shprits, Y. Y., D. Subbotin, and B. Ni (2009), Evolution of electron fluxes in the outer radiation belt computed with the VERB code, *J. Geophys. Res.*, *114*, A11209, doi:10.1029/2008JA013784.

Smith, M. J., D. A. Bryant, and T. Edwards (1980), Pulsations in auroral electrons and positive ions, *J. Atmos. Terr. Phys.*, *42*, 167–178, doi:10.1016/0021-9169(80)90077-X.

Smith, R. L. (1961), Propagation characteristics of whistlers trapped in field-aligned columns of enhanced ionization, *J. Geophys. Res.*, *66*, 3699–3707, doi:10.1029/JZ066i011p03699.

Streltsov, A. V., M. Lampe, W. Manheimer, G. Ganguli, and G. Joyce (2006), Whistler propagation in inhomogeneous plasma, *J. Geophys. Res.*, *111*, A03216, doi:10.1029/2005JA011357.

Subbotin, D., Y. Shprits, and B. Ni (2010), Three-dimensional VERB radiation belt simulations including mixed diffusion, *J. Geophys. Res.*, *115*, A03205, doi:10.1029/2009JA015070.

Summers, D., C. Ma, N. P. Meredith, R. B. Horne, R. M. Thorne, D. Heynderickx, and R. R. Anderson (2002), Model of the energization of outer-zone electrons by whistler-mode chorus during the October 9, 1990 geomagnetic storm, *Geophys. Res. Lett.*, *29*(24), 2174, doi:10.1029/2002GL016039.

Takahashi, K., C. Z. Cheng, R. W. McEntire, and L. M. Kistler (1990), Observation and theory of Pc 5 waves with harmonically related transverse and compressional components, *J. Geophys. Res.*, *95*, 977–989, doi:10.1029/JA095iA02p00977.

Thorne, R. M., T. P. O'Brien, Y. Y. Shprits, D. Summers, and R. B. Horne (2005), Timescale for MeV electron microburst loss during geomagnetic storms, *J. Geophys. Res.*, *110*, A09202, doi:10.1029/2004JA010882.

Thorne, R. M., B. Ni, X. Tao, R. B. Horne, and N. P. Meredith (2010), Scattering by chorus waves as the dominant cause of diffuse auroral precipitation, *Nature*, *467*, 943–946, doi:10.1038/nature09467.

Tsurutani, B. T., and E. J. Smith (1974), Postmidnight chorus: A substorm phenomenon, *J. Geophys. Res.*, *79*, 118–127, doi:10.1029/JA079i001p00118.

Zhu, X., and M. G. Kivelson (1991), Compressional ULF waves in the outer magnetosphere: 1. Statistical study, *J. Geophys. Res.*, *96*, 19,451–19,467.

V. Angelopoulos, Institute of Geophysics and Planetary Physics, Department of Earth and Space Sciences, University of California, Los Angeles, CA 90095-1567, USA. (vassilis@ucla.edu)

J. Bortnik, L. Chen, W. Li, Y. Nishimura, and R. M. Thorne, Department of Atmospheric and Oceanic Sciences, University of California, 405 Hilgard Ave., Los Angeles, CA 90095-1565, USA. (jbortnik@gmail.com; clj@atmos.ucla.edu; moonli@atmos.ucla.edu; toshi@atmos.ucla.edu; rmt@atmos.ucla.edu)